Tetrahedron Letters 50 (2009) 3418–3421

Contents lists available at ScienceDirect

Tetrahedron Letters

journal homepage: www.elsevier.com/locate/tetlet

Synthesis and characterization of a new prostaglandin H synthase model

Jakkidi J. Reddy, Takehiro Ohta, Yoshinori Naruta *

Institute for Materials Chemistry and Engineering (IMCE), Kyushu University, 6-10-1 Hakozaki, Higashi-ku, Fukuoka 812-8581, Japan

ARTICLE INFO

Article history:
Received 15 January 2009
Revised 17 February 2009
Accepted 19 February 2009
Available online 25 February 2009

ABSTRACT

Prostaglandin H synthases (PGHSs) are heme-containing enzymes, which directly add two O_2 molecules to arachidonic acid (AA) by the initiation of H-atom abstraction of 1,4-diene moiety and through sequential reactions to give PGH_2 as a final product. Here, we report the synthesis of a new PGHS model, which has two binaphthol bridges in one side of an iron porphyrin. Its substrate reaction site is more flexible and accordingly less hindered than the previous four binaphthol-bridged twin-coronet-type models (FeTCP). The present model is expected to accept higher olefins, which can reach the intermediate phenoxyl radical and iron in this complex. Upon treatment of the iron complex with *m*CPBA at −50 °C, we succeeded in the quantitative generation of the corresponding naphthoxyl radical, which was characterized by the increase in characteristic absorbance for naphthoxyl radical at 385 and 485 nm as well as by its ESR signal and recovery of the original spectra by the addition of *N*,*N*-dimethylaniline as an efficient reducing agent.

1. Introduction

Tyrosyl radical acts as a mediator for electron/proton transfer reactions coupled to metal redox centers in various metalloenzymes, such as photosystem II in plant chloroplast and prostaglandin H synthases (PGHSs) in spite of its instability under aerobic conditions.[1] PGHSs are a family of typical tyrosyl-radical-mediating enzymes and catalyze the addition of two oxygen molecules to arachidonic acid (AA) to form prostaglandin H_2 (PGH_2) through multi-step reactions in 'one pot'. The tyrosyl residue (Tyr385 for PGHS-1) in PGHS locates 10 Å from the heme unit in the peroxidase active site.[2] PGHS is a bifunctional enzyme[3] that catalyzes two essential reactions, (1) generation of the tyrosyl radical (Tyr-O·) by a rapid intramolecular electron transfer from tyrosine to an oxo-iron(IV) porphyrin π-cation radical and (2) regio- and stereoselective H radical abstraction of the 13-*pro-S* hydrogen from AA and trapping of the resultant radical with O_2.[4] The succeeding cyclization, the addition of another O_2 atom, and hydrogen atom abstraction from the resultant Tyr-OH furnish the formation of PGH_2.

However, the intrinsic instability of aryloxyl radicals makes the development of aryloxyl-radical-mediated reactions difficult in organic synthesis[5] in spite of its potential utility, because of their easy oxidation by oxygen molecule or radical coupling between two radicals without any (steric) protection of the phenoxyl radicals. By inspection of the environment around the tyrosyl residue in PGHS, the key for the utilization of any phenoxyl radicals for organic synthesis is the avoidance of radical coupling and O_2 oxidation, that is, the suitable block of the radical centers on the phenoxyl radicals. Based on the analysis, we have reported an active site model 'twin-coronet'[6] porphyrin (FeTCP)[7] as a PGHS model (Fig. 1), where we used a substituted binaphthol as a phenoxyl

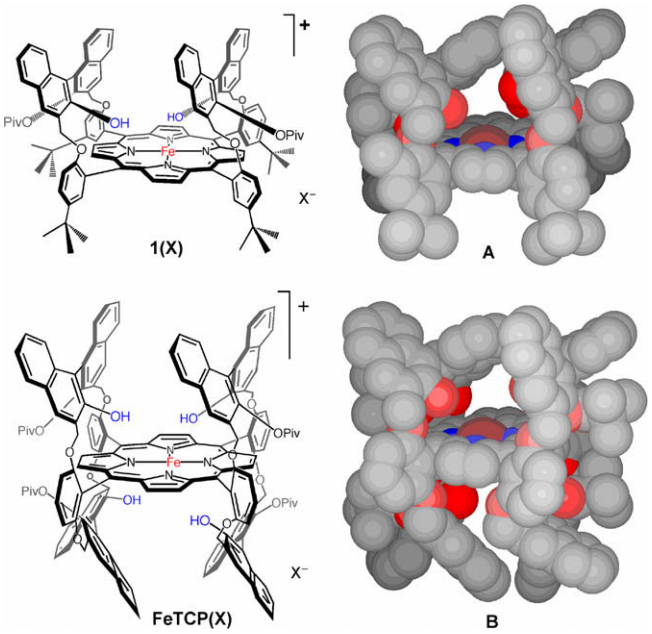

Figure 1. A new *syn*-binaphthol-bridged iron porphyrin [**1**(**X**)] and its computer-generated model (A), where the counter anion is omitted. Reported FeTCP(X) and its structural model (B). Piv = pivaloyl.

* Corresponding author. Tel./fax: +81 (0) 92 642 2731.
E-mail address: naruta@ms.ifoc.kyushu-u.ac.jp (Y. Naruta).

0040-4039/$ - see front matter © 2009 Elsevier Ltd. All rights reserved.
doi:10.1016/j.tetlet.2009.02.145

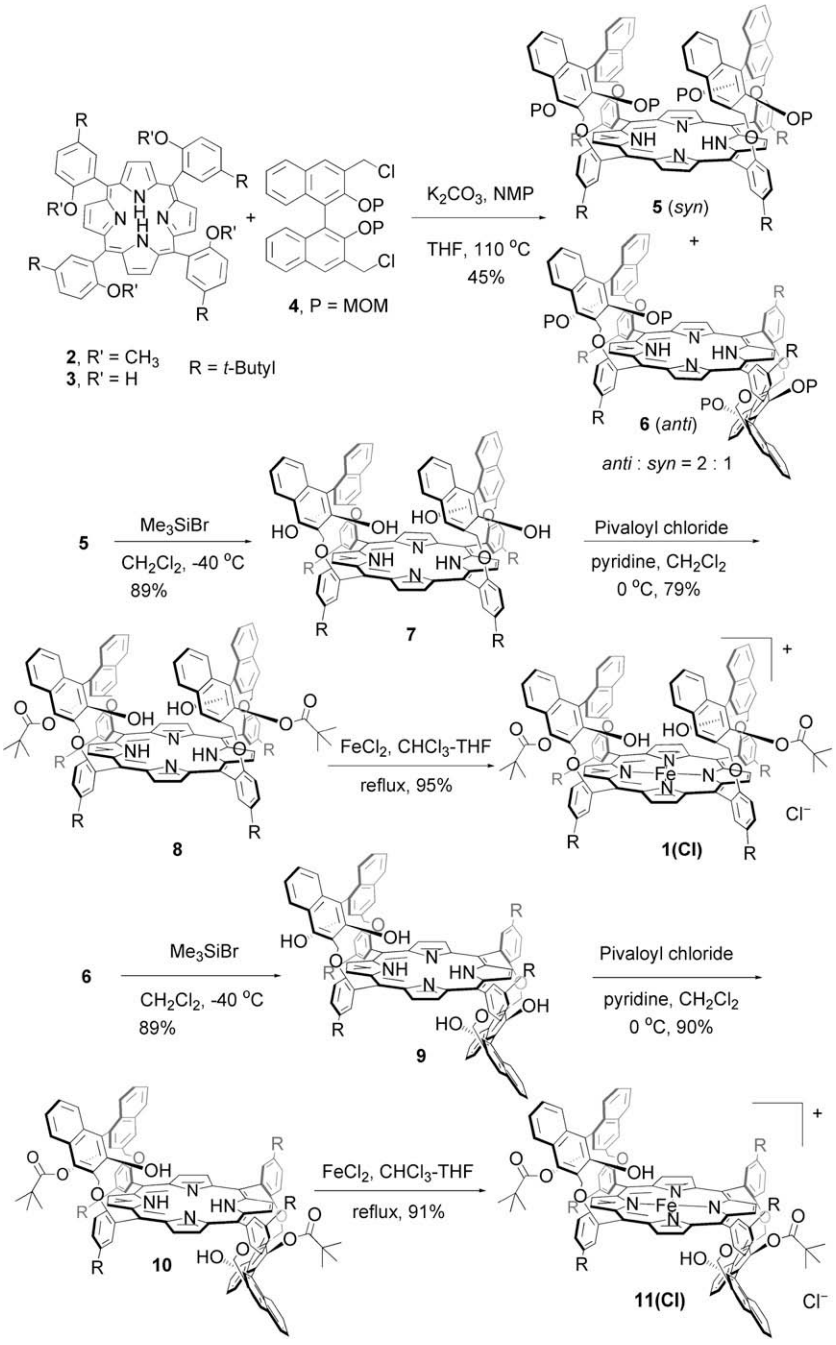

Scheme 1.

radical equivalent fixed on an iron porphyrin by bridging between adjacent *meso*-phenyl groups. We designed so that the two adjacent and para positions of the binaphthol group, where electron density becomes higher than the other position in its aryloxyl radical. We successfully attained the observation of the corresponding intermediate naphthoxyl radical by *m*CPBA oxidation and realized the catalytic oxygenation reaction of *cis*,*cis*-1,4-diene in high stereoselectivity. This is the first example of a model system utilizing the unstable Ar-O· radical as a mediator in catalytic oxygenation reactions and it provides important insights into the catalytic oxygenation mechanism of PGHSs. FeTCP has sterically blocked cavity by two binaphthol bridges on each face of the porphyrin ring. Though such solid structure enhances the radical stability, the steric hindrance around the cavities considerably reduces its reactivity and accordingly its applicability to various polyenes including AA.

Here, we report the synthesis and characterization of a new chemical model [**1**(**X**)] of PGHSs (Fig. 1), where only two binaphthol groups are bridged on the same side of the porphyrin ring, in order to increase the cavity motion. This design of the model complex also allows to keep the symmetry at the porphyrin synthetic stage.

The model synthesis was done according to Scheme 1. The starting porphyrin **2** was prepared by Lindsey method[8] (CH_2Cl_2, with $BF_3{\cdot}OEt_2$ catalyst in 42% yield) followed by demethylation with pyridinium hydrochloride at 240 °C (90%). The bridging of two MOM-protected optically active 1,1′-binaphthol-3,3′-dimethylene group to give **5** (syn) and **6** (anti) in 1:2 ratio (overall 45%

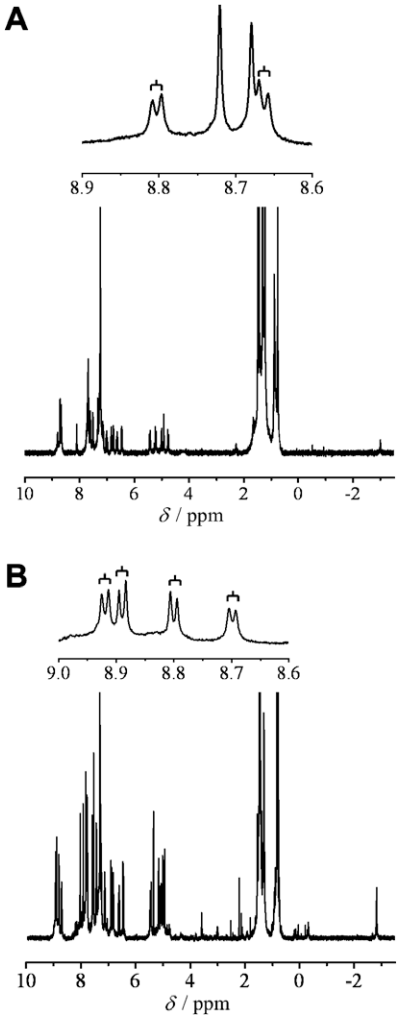

Figure 2. ^{1}H NMR of binaphthol-bridged model: (A) *anti*-isomer (**10**) and (B) *syn*-isomer (**8**). Each pyrrole β-protons are shown in each magnified spectra, J = 4.6 Hz.

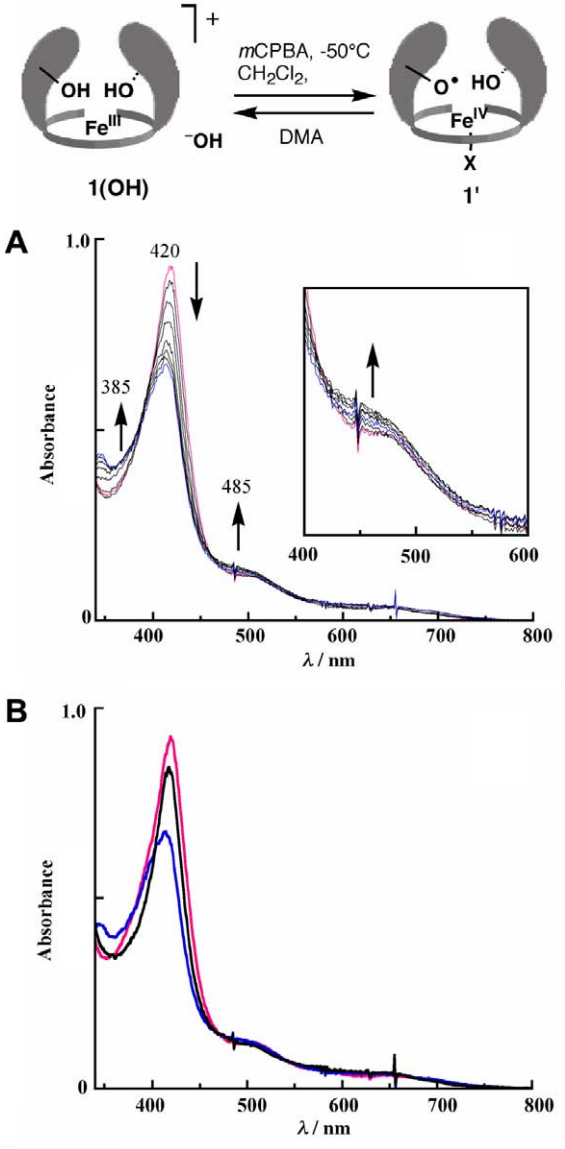

Figure 3. UV–vis spectral change of complex **1**(**OH**) to its oxidized form (**1**′) upon treatment with *m*CPBA: (A) Time course of the spectral change (20 s interval). Inset: magnified spectra of the 400–600 nm region. (B) Comparison of the spectra of complex **1**(**OH**) before oxidation (red), complex **1**′ (after oxidized) (blue), and recovery of **1**(**X**) by the addition of *N*,*N*-dimethylaniline (black).

yield). Though we used the atropisomeric mixture of **3** for this binaphthol bridging reaction, it is interesting that the resultant-bridged complexes, **5** and **6**, are obtained in a high yield. The two isomers were separated by column chromatography. Both *syn*- and *anti*-isomers can be distinguished by ^{1}H NMR spectra of their pyrrole β-protons by inspection of their molecular symmetry (Fig. 2): In *syn*-isomer (**5**), each couple of adjacent β protons on each pyrrole ring is in different environment, thus, they give four doublets. The *anti*-isomer (**6**) has two sets of equivalent pyrrole β-protons and each two protons of two pyrrole rings below the naphthalene bridges are in different environment. Thus, *anti*-isomer shows two singlets and two doublets.

syn-Isomer (**5**) was transformed to complex **1**(**Cl**) by deprotection of MOM group with TMSBr and selectively protected its outer two hydroxyl groups by pivaloyl group with pivaloyl chloride followed by metallation with $FeCl_2$. Complex **1**(**Cl**) and intermediates are fully characterized by ^{1}H NMR and HRMS. Similarly, *anti*-isomer was also converted to the corresponding Fe complex **11**(**Cl**).

The oxidation of complex **1**(**OH**) (Fe^{III}), transferred by the base treatment of **1**(**Cl**), with *m*-chloroperbenzoic acid (*m*CPBA, 2.5 M equiv) in CH_2Cl_2 at −50 °C indicated the quick spectral change showing clear isosbestic points and increase in absorbance at 385 and 485 nm (Fig. 3A). The bands at 385 and 485 nm are assigned to be the corresponding naphthoxyl radical (Np-O·) based on comparison of the spectroscopic evidences reported for naphthoxyl radical by us[6] (for FeTCP, λ = 365 (sh) and 478) and Nath and Neta[9] (for 2-Np-O·, 335 and 480 nm). The formation of Np-O· was further confirmed by its EPR signal,[†] g = 2.0046, which was exactly same as the reported one for FeTCP.[6] The oxidized species **1**′ also exhibits absorption bands at 420 (Soret) and 510 nm (Q), which are characteristic of an Fe^{IV}(=O) porphyrin (compound II)[10] and differentiated from $Fe^{IV}\mathbf{P}^{+\cdot}$ (compound I).[11] Thus, the new species **1**′ is assigned to be compound II with NpO·, [Fe^{IV}(=O)**P**(Np-O·)] (**P** = porphyrin). To confirm its oxidation state, addition of *N*,*N*-dimethylaniline (DMA) as an efficient single-electron-reducing agent[12] showed the recovery of the UV–vis spectra as the starting Fe^{III} species [**1**(**X**)].

It is worth to mention on the rapid formation of the oxidized form **1**(**OH**) upon treatment with *m*CPBA. Within 10 min after *m*CPBA addition, the spectral change to **1**′ is completed. However,

[†] Conditions: 9.19 GHz, microwave frequency: 100 KHz, modulation width: 0.5 mT, microwave power: 1 mW, temperature: 77 K.

the previous model, FeTCP, took at least 30 min for the complete conversion to the corresponding oxidized form even at higher temperature (−40 °C) at the same concentration. This proves the new model **1**(**X**) has less sterically hindered reaction site than FeTCP.

In conclusion, we synthesized and characterized a binaphthol-bridged porphyrin as a new PGHS model successfully. Its species that was oxidized by *m*CPBA was identified as [Fe^{IV}(=O)**P**(Np-O·)] from its UV–vis spectra as well as from the recovery by the reduction with DMA.[12] The higher reactivity of **1**(**X**) with *m*CPBA is promising to apply it to polyene oxygenation. The use of **1**(**X**) and **11**(**X**) as PGHS model catalysts and comparison of their reactivity are now underway.

2. Spectral data for selected compounds

2.1. Compound 8 (*syn*)

^{1}H NMR ($CDCl_3$, 400 MHz): δ8.92 (d, 2H, *J* = 4.6 Hz, pyrrole β-H), 8.88 (d, 2H, *J* = 4.6 Hz, pyrrole β-H), 8.80 (d, 2H, *J* = 4.6 Hz, pyrrole β-H), 8.69 (d, 2H, *J* = 4.6 Hz, pyrrole β-H), 8.02 (d, 2H, *J* = 2.6 Hz, Ar-H), 7.91 (d, 4H, *J* = 2.6 Hz, Ar-H), 7.83–7.64 (m, 4H, Ar-H), 7.57 (d, 4H, *J* = 8.3 Hz, Ar-H), 7.53 (s, 4H, Ar-H), 7.43 (d, 2H, *J* = 8.3 Hz, Ar-H), 7.37–7.23 (m, 2H, Ar-H), 7.13 (t, 2H, *J* = 8.3 Hz, Ar-H), 6.88 (d, 2H, *J* = 9.5 Hz, Ar-H), 6.82 (t, 2H, *J* = 7.5 Hz, Ar-H), 6.60 (t, 2H, *J* = 9.5 Hz, Ar-H), 6.45 (d, 2H, *J* = 8.5 Hz, Ar-H), 5.45 (d, 2H, *J* = 12.9 Hz, benzylic), 5.16 (d, 2H, *J* = 9.2 Hz, benzylic), 5.08 (d, 2H, *J* = 12.9 Hz, benzylic), 4.99 (d, 2H, *J* = 9.2 Hz, benzylic), 4.94 (s, 2H, OH), 1.46 (s, 36H, *t*-butyl-CH_3), 0.82 (s, 18H, *t*-butyl-CH_3), −2.84 (s, 2H, N–H). HR-MS (FAB, NBA): Found: *m/z* 1690.789. Calcd for $C_{114}H_{106}N_4O_{10}$: 1690.790.

2.2. Compound 10 (*anti*)

^{1}H NMR ($CDCl_3$, 400 MHz): δ8.80 (d, 2H, *J* = 4.6 Hz, pyrrole β-H), 8.70 (s, 2H, pyrrole β-H), 8.67 (s, 2H, pyrrole β-H), 8.65 (d, 2H, *J* = 4.6 Hz, pyrrole β-H), 8.10 (d, 2H, *J* = 2.4 Hz, Ar-H), 7.75–7.64 (m, 4H, Ar-H), 7.51 (d, 2H, *J* = 3.4 Hz, Ar-H), 7.46 (d, 4H, *J* = 3.4 Hz, Ar-H), 7.34 (s, 4H, Ar-H), 7.28–7.21 (m, 4H, Ar-H), 7.14 (t, 2H, *J* = 7.5 Hz, Ar-H), 7.02 (dd, 2H, *J* = 7.0, 5.6 Hz, Ar-H), 6.84 (t, 2H, *J* = 7.0 Hz, Ar-H), 6.78 (d, 2H, *J* = 8.0 Hz, Ar-H), 6.63 (t, 2H, *J* = 6.5 Hz, Ar-H), 6.46 (d, 2H, *J* = 8.5 Hz, Ar-H), 5.43 (d, 2H, *J* = 12.2 Hz, benzylic), 5.22 (d, 2H, *J* = 12.2 Hz, benzylic), 5.01 (d, 2H, *J* = 9.7 Hz, benzylic), 4.92 (s, 2H, OH), 4.76 (d, 2H, *J* = 9.7 Hz, benzylic), 1.43, 1.32, 1.23 (3s, 36H, *t*-butyl-CH_3), 0.76 (s, 18H, *t*-butyl-CH_3), −2.99 (s, 2H, N–H). HR-MS (FAB, NBA, $C_{114}H_{106}N_4O_{10}$): Found: *m/z* 1690.790. Calcd for $C_{114}H_{106}N_4O_{10}$: 1690.790.

Acknowledgment

J.J.R. thank to JSPS for financial support as a JSPS postdoctoral fellow.

Supplementary data

Supplementary data associated (detailed experimental procedure, spectroscopic data) with this article can be found, in the online version, at doi:10.1016/j.tetlet.2009.02.145.

References

1. Pesavento, R. P.; van der Donk, W. A. *Adv. Protein Chem.* **2001**, *58*, 317–385; Stubbe, J.; van der Donk, W. A. *Chem. Rev.* **1998**, *98*, 705–762; Haruta, M. *Nature* **2005**, *437*, 1098.
2. Marnett, L. J.; Rowlinson, S. W.; Goodwin, D. C.; Kalgutkar, A. S.; Lanzo, C. A. *J. Biol. Chem.* **1999**, *274*, 22903–22906; Smith, W. L.; DeWitt, D. L.; Garavito, R. M. *Annu. Rev. Biochem.* **2000**, *69*, 145–182.
3. Fillimonov, I. S.; Vrzheshch, P. V. *Biochemistry (Moscow)* **2007**, *72*, 944–953.
4. Dietz, R.; Nastainczyk, W.; Ruf, H. H. *Eur. J. Biochem.* **1988**, *171*, 321–328; Peng, S.; Okeley, N. M.; Tsai, A.-L.; Wu, G.; Kiulmacz, R. J.; van der Donk, W. A. *J. Am. Chem. Soc.* **2002**, *124*, 10785–10796.
5. Chaudhuri, P.; Hess, M.; Müller, J.; Hildenbrand, K.; Bill, E.; Weyhermüller, T.; Wieghardt, K. *J. Am. Chem. Soc.* **1999**, *121*, 9599–9610.
6. Matsui, E.; Naruta, Y.; Tani, F.; Shimazaki, Y. *Angew. Chem., Int. Ed.* **2003**, *42*, 2744–2747; Matsui, E.; Naruta, Y.; Tani, F.; Shimazaki, Y. *Angew. Chem.* **2003**, *115*, 2850–2853.
7. Matsu-ura, M.; Tani, F.; Nakayama, S.; Nakamura, N.; Naruta, Y. *Angew. Chem.* **2000**, *112*, 2083–2086; Matsu-ura, M.; Tani, F.; Nakayama, S.; Nakamura, N.; Naruta, Y. *Angew. Chem., Int. Ed.* **2000**, *39*, 1989–1991; Tani, F.; Matsu-ura, M.; Nakayama, S.; Ichimura, M.; Nakamura, N.; Naruta, Y. *J. Am. Chem. Soc.* **2001**, *123*, 1133–1142; Matsu-ura, M.; Tani, F.; Naruta, Y. *J. Am. Chem. Soc.* **2002**, *124*, 1941–1950.
8. Lindsey, J. S.; Schreiman, I. C.; Hsu, H. C.; Kearney, P. C.; Marguerettaz, A. M. *J. Org. Chem.* **1987**, *52*, 827–836.
9. Nath, T.; Neta, P. *J. Phys. Chem. A* **1998**, *102*, 7081–7085.
10. Groves, J. T.; Gross, Z.; Stern, M. K. *Inorg. Chem.* **1994**, *33*, 5065–5072.
11. Fujii, H.; Yoshimura, T.; Kamada, H. *Inorg. Chem.* **1996**, *35*, 2373–2377.
12. Karki, S. B.; Dinnocenzo, J. P.; Jones, J. P.; Korzekwa, K. R. *J. Am. Chem. Soc.* **1995**, *117*, 3657–3664.